Water Interactions with Actinide Oxides from First Principles:

A Computational Study – 16470

Bengt Tegner *, Andrew Kerridge **, Nikolas Kaltsoyannis *
* The University of Manchester, Oxford Road, Manchester, M13 9PL, UK
** Lancaster University, Bailrigg, Lancaster, LA1 4YW, UK

ABSTRACT

The interactions between water and the actinide oxides UO_2 and PuO_2 are important when considering the long-term storage of spent nuclear fuel. However, experimental studies in this area are severely limited by plutonium's intense radioactivity, and hence we have recently begun to investigate these interactions computationally. In this contribution we report the results of first principles calculations of the electronic and geometric structures of AnO_2 bulk, AnO_2 clusters, and AnO_2 surfaces (An = U, Np, Pu), as well as the interaction of water with the latter. Strongly-correlated effects are taken into account using a Hubbard corrected potential, which enables us to perform efficacious plane-wave density functional calculations of extended systems. In particular, we compare results of water adsorption on UO_2 (111) with the corresponding results on CeO_2, focusing on the energetics and structural properties of molecular versus dissociative adsorption, for both partially and fully covered surfaces.

INTRODUCTION

One of the problems with nuclear energy is the long term storage of nuclear waste, spent nuclear fuel and the products of fuel reprocessing. Our particular project concerns the civilian stores of highly radioactive plutonium dioxide. Presently, the UK's PuO_2 is stored as a powder in stainless steel storage containers, while the government decides its long term fate. However, some of these steel containers have started to buckle, leading to the hypothesis that gas build up, possibly from water vapor due to desorption or the production of hydrogen gas due to the radiolysis of water, causes some of the containers to pressurize. We are exploring these suggestions computationally.

Standard plane-wave density functional theory (DFT) using the local density approximation (LDA) or the generalized gradient approximation (GGA) predicts a metallic ground state for AnO_2 (An = U, Np, Pu). This is by contrast to experiments, where they are all found to be insulators, with a bandgap of about 2 - 3 eV. The reason for this discrepancy is the failure of both of these approximations to fully describe the localized nature of the electronic *5f* states present in the actinides. One way around this problem is to introduce a Hubbard-type potential to the system which penalizes delocalized states and forces the *5f* electrons to be localized on the actinide ion. This approach is called DFT+*U* and has been used successfully on a number of strongly-correlated systems [18-22]. The actual values of the Hubbard Coulomb (*U)* and exchange (*J)* parameters are typically derived from experimental data, such as by

fitting to the experimental band gap. Below is a brief summary of previous DFT+*U* results on the actinide oxides.

Dudarev *et al.* [1] studied UO_2 using LDA+*U* with the parameters *U* = 4.5 eV and *J* = 0.54 eV. The parameters were fitted from 'experimental considerations'. They found UO_2 to be a Mott-Hubbard insulator with a calculated band gap of 1.1 eV.
Yun *et al.* [2] studied UO_2 using GGA+*U* also with the parameters *U* = 4.5 eV and *J* = 0.5 eV, following Dudarev's DFT+*U* formalism. They also found UO_2 to be a Mott-Hubbard insulator, this time with a band gap of 1.8 eV. Additionally, Yu *et al.* [3] studied UO_2 using GGA+*U* with the parameters *U* = 4.772 eV and *J* = 0.511 eV to match the experimental band gap, using a similar approach to Yun et al. They too found UO_2 to be a Mott-Hubbard insulator, with a band gap of 2.1 eV (the experimental value).

Wang *et al.* [4] explored NpO_2 using LDA+*U*, varying the *U* parameter to match the lattice constant and band gap, using Dudarev's DFT+*U* formalism. Using *U* = 4.0 eV and *J* = 0.6 eV, they found NpO_2 to be a Mott-Hubbard insulator with a band gap of 2.2 eV. Furthermore, Wen *et al.* [8], studied NpO_2 using GGA+*U*, with *U* = 4.5 eV and *J* = 0.5 eV. By contrast to earlier studies, they found NpO_2 to be a charge-transfer insulator with a band gap of 2.6 eV.

Sun *et al.* [5] studied PuO_2 using LDA+*U*, varying *U* to match the band gap, using Dudarev's DFT+*U* formalism. With *U* = 4.75 eV and *J* = 0.75 eV, they found PuO_2 to be a charge-transfer insulator with a band gap of 1.5 eV. Additionally, Jomard *et al.* [6] probed PuO_2 using PBE+*U*, varying *U* to match the band gap, using Lichtenstein's DFT+*U* formalism [7]. Using *U* = 4.0 eV and *J* = 0.70 eV, they found PuO_2 to be a charge-transfer insulator with a band gap of 1.5 eV. Moreover, Wen *et al.* [8] studied PuO_2 using LDA+*U* and GGA+*U*, with the parameters *U* = 4.5 eV and *J* = 0.5 eV. They found PuO_2 to be a charge-transfer insulator with a band gap of 1.6 eV, in agreement with earlier work by Jomard *et al*. [6].

METHODS

Periodic calculations

The crystal structure of the actinide oxides is shown in Figure 1. They all adopt the fluorite (CaF_2) structure, with the actinide ions (gray) occupying the face-centered cubic sites and the oxygen ions (red) occupying the tetrahedral holes.

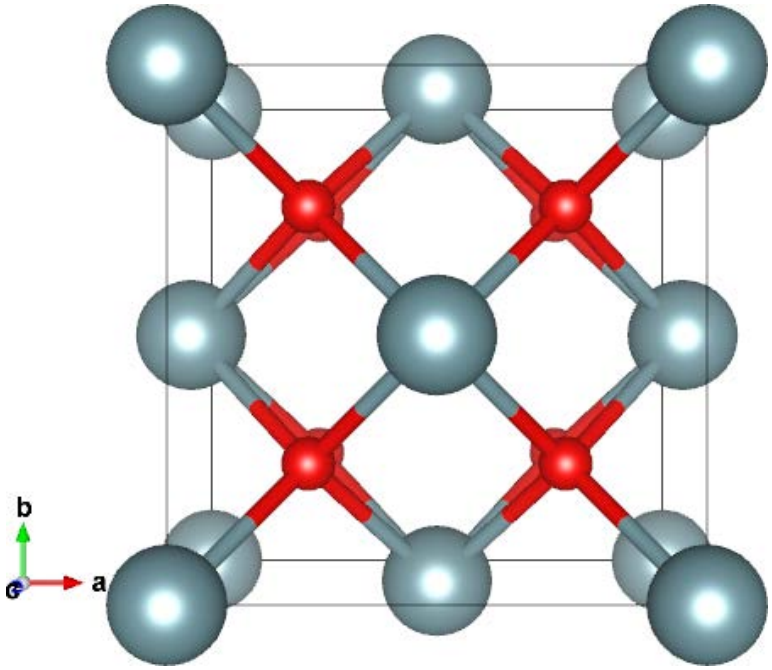

Fig 1: AnO_2 crystal structure. The actinide ions are gray and the oxygen atoms are red.

The calculations were performed using VASP 5.3.5 [9-12], a plane-wave DFT code using Projector-Augmented Wave (PAW)-pseudopotentials [13, 14] to describe the ions and employing Monkhorst-Pack (MP) [15] grids for the *k*-space integration. All calculations used a plane wave cut-off of 650 eV and an MP-grid spacing of 0.1 $Å^{-1}$ for the Brillouin zone sampling. The generalized gradient approximation of Perdew, Burke, and Ernzerhof (PBE) [16, 17], with and without a Hubbard correction [1, 7], was used for the exchange-correlation. A tetragonal unit cell of 12 atoms was used for the bulk system.

Cluster calculations

Rather than fitting the *U* and *J* parameters to experimental data, we have attempted to calculate them from first principles using a modified version of the molecular code GAMESS-US, an approach developed by Mosey *et al*. [18, 19] for transition metal oxides. The actinide ions are embedded in a molecular cluster of oxygen anions and other metal cations, making a neutral cluster whilst mimicking the local chemical environment in the solid. A ball and stick image of a small cluster is shown in Figure 2 below.

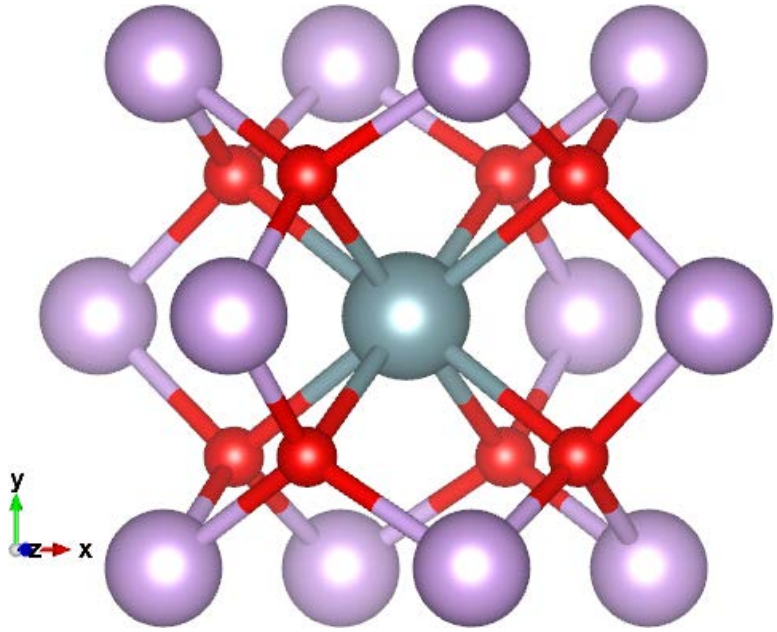

Fig 2: NpO_8Na_{12} molecular cluster with a single Np atom (gray), eight oxygen atoms (red) and twelve sodium atoms (purple), arranged to mimic the local chemical environment of the solid. The Na atoms are chosen to balance the charge.

This cluster is then geometrically and electronically relaxed at the unrestricted Hartree-Fock level of theory and the *U* and *J* parameters are derived from the converged electronic structure.

DISCUSSION

The *U* and *J* parameters derived from different molecular clusters are shown in Table I below.

TABLE I: Hubbard parameters derived from cluster calculations.

Cluster	*U*	*J*	*U – J*
UO_2^{2+}	13.3038	0.4451	12.8587
NpO_2^{2+}	19.3933	0.7568	18.6365
$UO_2^{2+} \bullet 5\ H_2O$	10.4284	0.4467	9.9818
$NpO_2^{2+} \bullet 5\ H_2O$	16.1516	0.7711	15.3804
NpO_8Na_{12}	19.9733	0.7853	19.1880

Studying Table I and focusing on uranyl and neptunyl, we find that the *U* and *J* values decrease on going from the bare dications to the ions complexed with five water

molecules in the equatorial plane. This decrease with increasing cluster size is in agreement with previous work on transition metal oxides by Mosey et al. [18, 19] who find that *U* and *J* converge to smaller values when using larger clusters. We have attempted to converge *U* and *J* for Np by initially calculating a neptunium cluster (Figure 2) and then moving to clusters with more than one Np. While the NpO_8Na_{12} cluster yielded *U* and *J* values (table I), we could not obtain convergence of the electronic self-consistent field for the larger clusters.

The data in Table I show that the values of *U* and *J* obtained from these molecular clusters are much larger than those used in the GGA+*U* approach by other workers. Using larger *U* and *J* values within the PBE+*U* scheme produces some peculiar results. For example, studying bulk NpO_2 using U_{eff} = (i.e. $U - J$) = 9.9 eV, we find NpO_2 to be a charge-transfer insulator with a bandgap of 4.1 eV, far bigger than previous studies. Furthermore, the corresponding results for UO_2 and PuO_2 are equally erroneous. As we cannot obtain electronic structures for multi-metallic molecular clusters (which might be expected to produce smaller values of *U* and *J*), we have decided to revert to using values closer to those reported previously in the literature.

Lattice parameters

The calculated lattice parameters for the three oxides in the antiferromagnetic (AFM) state using 12-atom tetragonal unit cells, and using *U* = 4.5 eV and *J* = 0.5 eV, are shown in Table II below. We find that whilst the general trend corresponds well with experimental data, PBE+*U* overestimates the lattice parameter for all three oxides by up to 1.75 %, in agreement with previous studies summarized by Wen et al. [8].

TABLE II: Calculated lattice parameters for AnO_2 (An = U, Np, Pu).

System	PBE+*U*	Other Calcs. (PBE+*U*, *HSE* [8])	Expt. [8]
UO_2	5.566	5.568, *5.458*	5.470
NpO_2	5.498	5.498, *5.412*	5.420
PuO_2	5.435	5.465, *5.383*	5.398

Densities of state and band gaps

The calculated densities of states (DOS) for the three oxides using *U* = 4.5 eV and *J* = 0.5 eV are shown in Figure 3 and the resulting electronic band gaps are given in Table III. We find that the calculated band gap for NpO_2 agrees reasonably well with experiment, however we overestimate the bandgap for UO_2 and underestimate it for PuO_2. This again is in agreement with previous computational studies [8].

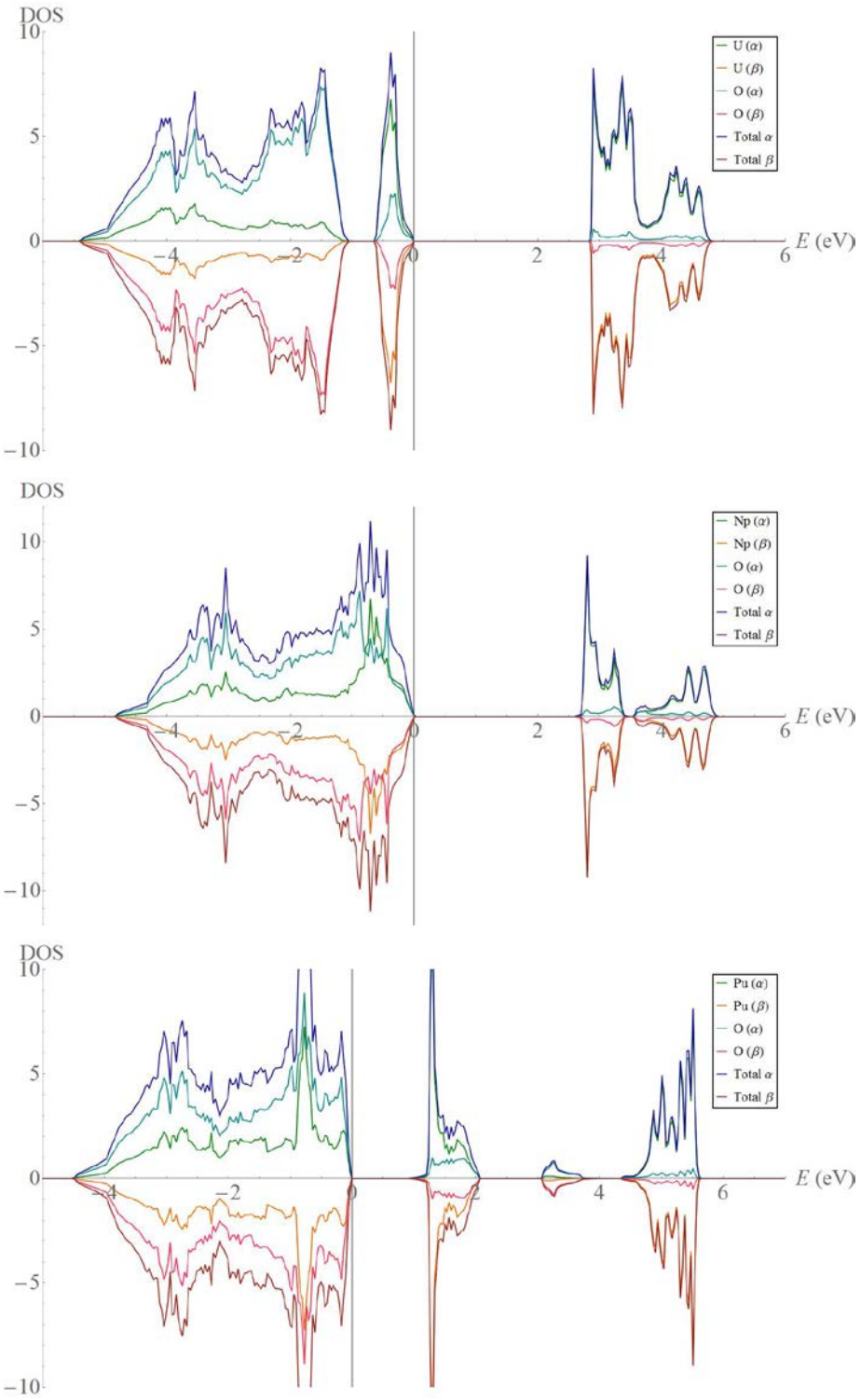

Fig 3: Electronic densities of states for AnO_2 (An = U (upper), Np (middle), Pu) in the anti-ferromagnetic state. The positive values represent the spin-up states and the negative values represent the spin-down states.

TABLE III: Band gaps (eV) for AnO_2 (An = U, Np, Pu).

System	PBE+*U*	Other Calcs. (PBE+*U*, *HSE* [8])	Expt. [8]
UO_2	2.8	2.3, *2.4*	2.1
NpO_2	2.6	2.6, *2.4*	2.80
PuO_2	1.3	1.6, *2.4*	2.85

Water adsorption

We now turn to water adsorption energies on the UO_2 (111) surface. The system studied is shown schematically in Figure 4 below. The system consists of a repeating slab of 16 UO_2 units arranged in four layers with 18 Å of vacuum between each slab.

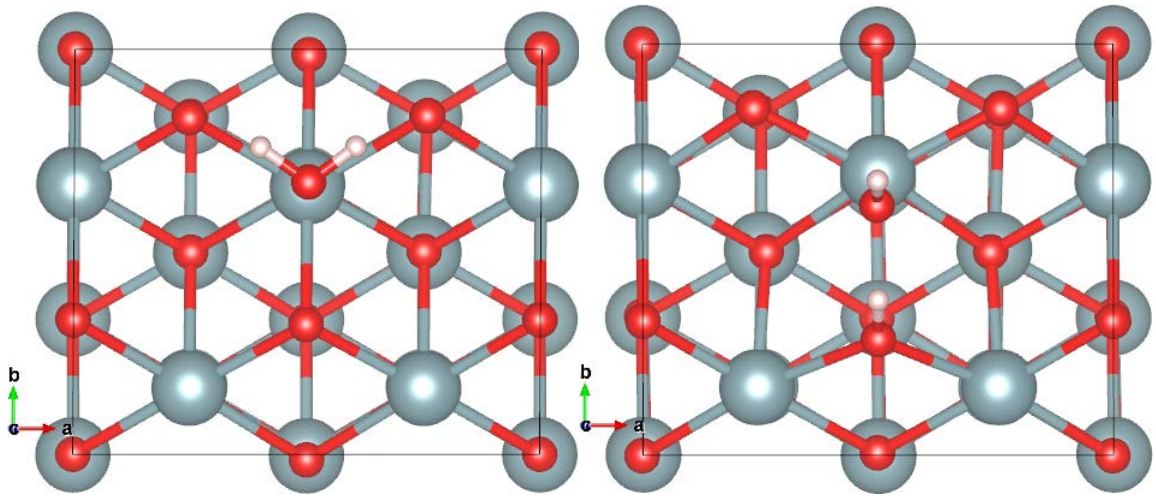

Fig 4: Single water molecule adsorbed molecularly (left) and dissociatively (right) on the 2 × 2 UO_2 (111) surface, yielding a coverage of 25%, *i.e.* ¼ of a monolayer. U atoms in gray, oxygen in red and hydrogen in white.

The calculated adsorption energies of molecularly and dissociatively adsorbed water on UO_2 (Figure 4) are shown in Table IV. Corresponding data on CeO_2 from Molinari and coworkers [22] are shown for comparison, and selected interatomic distances are shown in Table V. Comparing the data, we find close similarity between CeO_2 and UO_2, particularly at full coverage. This strengthens the idea of using CeO_2 as a non-radioactive analog of the actinide oxides for experimental water adsorption studies.

TABLE IV: Water adsorption energies (eV) per molecule on the UO_2 (111) surface, and results for CeO_2 from Molinari *et al.* [22].

System	U_{eff} (eV)	0.25 ML	0.5 ML	0.75 ML	1.0 ML
UO_2 + H_2O	4.0	-0.53	-0.53	-0.53	-0.49
UO_2 + OH + H	4.0	-0.50	-0.41	-0.29	-0.15
CeO_2 + H_2O [22]	5.0	-0.56	-0.60	N/A	-0.57
CeO_2 + OH + H [22]	5.0	-0.59	N/A	N/A	-0.15

TABLE V: Selected interatomic distances for molecularly and dissociatively adsorbed water on the UO_2 (111) surface at coverages from 0.25 to 1.0 monolayers, and results for CeO_2 from Molinari *et al.* [22] H_W and O_W denote the hydrogen and oxygen atoms belonging to the water molecule whereas U_{1S}/Ce_{1S} and O_{1S} denote the outermost surface atoms.

Distance (Å)	UO_2 (0.25 – 1.0 ML)	CeO_2 (0.25 – 1.0 ML))[22]
H_W – O_{1S}	1.96 – 2.28	1.99 – 2.13
U_{1S} / Ce_{1S} – O_W	2.62 – 2.69	2.62
U_{1S} / Ce_{1S} – O_WH_W	2.18 – 2.26	2.22
U_{1S} / Ce_{1S} – $O_{1S}H_W$	2.33 – 2.44	2.41
$O_{1S}H_W$ – O_WH_W	1.61 – 2.39	1.65

CONCLUSIONS

To summarize, we find that modeling AnO_2 (An = U, Np, Pu) using DFT remains a challenge. That said, using the DFT+*U* approach with appropriate choice of the effective *U* parameter, we find that we can obtain structural and electronic properties of these oxides in broad agreement with previous work.

Water adsorption energies and distances on the UO_2 (111) surface look very similar to corresponding values on CeO_2, particularly at full coverage, strengthening the notion that CeO_2 can be used as an actinide oxide analog.

Moving on from the (111) surface, we will continue to study water adsorption on the (110) and (100) surfaces of all three target actinide oxides, before progressing to more complex systems such as reduced surfaces.

REFERENCES

[1] S. L. DUDAREV, D. NGUYEN MANH and A. P. SUTTON, *Philosophical Magazine Part B*, 75, 613 (1997).

[2] Y. YUN, H. KIM, H. LIM and K. PARK, *Journal of the Korean Physical Society*, 50, 1285, (2007).
[3] S.-W. YU, J. G. TOBIN, J. C. CROWHURST, S. SHARMA, J. K. DEWHURST, P. OLALDE-VELASCO, W. L. YANG and W. J. SIEKHAUS, *Phys. Rev. B,* 83, 165102, (2011).
[4] B.-T. WANG, H. SHI, W. LI and P. ZHANG, *Phys. Rev. B,* 81, 045119, (2010).
[5] B. SUN, P. ZHANG and X.-G. ZHAO, *J. Chem. Phys.,* 128, 084705, (2008).
[6] G. JOMARD, B. AMADON, F. BOTTIN and M. TORRENT, *Phys. Rev. B*, 78, 075125, (2008).
[7] A. I. LIECHTENSTEIN, V. I. ANISIMOV and J. ZAANEN, *Phys. Rev. B, 52, R5467*, (1995).
[8] X.-D. WEN, R. L. MARTIN, T. M. HENDERSON and G. E. SCUSERIA, *Chem. Rev.*, 113, 1063, (2013).
[9] G. KRESSE and J. HAFNER, *Phys. Rev. B*, 47, 558, (1993).
[10] G. KRESSE and J. HAFNER, *Phys. Rev. B*, 49, 14251, (1994).
[11] G. KRESSE and J. FURTHMÜLLER, *Comput. Mat. Sci.*, 6, 15, (1996).
[12] G. KRESSE and J. FURTHMÜLLER, *Phys. Rev. B*, 54, 11169, (1996).
[13] P. E. BLÖCHL, *Phys. Rev. B*, 50, 17953, (1994).
[14] G. KRESSE and D. JOUBERT, *Phys. Rev. B*, 59, 1758, (1999).
[15] H. J. MONKHORST and J. D. PACK, *Phys. Rev. B*, 13, 5188, (1976).
[16] J. P. PERDEW, K. BURKE and M. ERNZERHOF, *Phys. Rev. Lett.*, 77, 3865, (1996).
[17] J. P. PERDEW, K. BURKE and M. ERNZERHOF, *Phys. Rev. Lett.*, 78, 1396, (1997).
[18] N. J. MOSEY and E. A. CARTER, *Phys. Rev. B,* 76, 155123, (2007).
[19] N. J. MOSEY, P. LIAO and E. A. CARTER, *J. Chem.* Phys., 129, 014103, (2008).
[20] D. O. SCANLON, N. M. GALEA, B. J. MORGAN and G.W. WATSON, *J. Phys. Chem. C* 113, 11095, (2009).
[21] D. O. SCANLON, B. J. MORGAN and G.W. WATSON, *Phys. Chem. Chem. Phys*. 13, 4279, (2011).
[22] M. MOLINARI, S. C. PARKER, D. C. SAYLE and M. S. ISLAM, *J. Phys. Chem. C* 116:7073, (2012).

ACKNOWLEDGEMENTS
We would like to thank the EPSRC DISTINCTIVE consortium (http://www.distictiveconsortium.org) for funding, and Howard Sims at the National Nuclear Laboratory and Jeffrey Hobbs at Sellafield Ltd for helpful discussions.

We are also grateful for access to ARCHER, the UK's National Supercomputing Service (http://www.archer.ac.uk), *via* the HEC Materials Chemistry Consortium, which is funded by EPSRC (EP/L000202). We also thank University College London for computing resources *via* Research Computing's "Legion" cluster (Legion@UCL) and associated services, and the "Iridis" facility of the e-Infrastructure South Consortium's Centre for Innovation.